ARTICLE

The high-density lipoprotein receptor Scarb1 is required for normal bone differentiation in vivo and in vitro

Irina L. Tourkova[1,2] · Steven F. Dobrowolski[2] · Cassandra Secunda[2] · Mone Zaidi[3] · Ioanna Papadimitriou-Olivgeri[4] · Dionysios J. Papachristou[2,4] · Harry C. Blair[1,2]

Abstract

We examined bone formation and turnover in high-density lipoprotein (HDL) receptor, scavenger receptor type I (Scarb1), knockout animals relative to wild-type (WT) controls. Scarb1$^{-/-}$ animals have elevated serum adrenocorticotropic hormone (ACTH) due to the role of Scarb1 in glucocorticoid production, which might cause increased bone mass. However, this was not observed: Scarb1$^{-/-}$ mice, with ACTH, over 1000 pg/ml relative to wild-type ACTH ~ 25 pg/ml, bone of the knockout animals was osteopenic relative to the wild type at 16 weeks, including bone volume/total volume and trabecular thickness. Other serum parameters of WT and Scarb1$^{-/-}$ animals in cortisol or calcium were unaffected, although Scarb1$^{-/-}$ animals had significantly elevated PTH and decreased phosphate. Osteoblast and osteoclast-related mRNAs extracted from bone were greatly decreased at 8 or 16 weeks. Importantly, in normal ACTH, osteogenic differentiation in vitro from mesenchymal stem cells showed reduced alkaline phosphatase and mineralization. In Scarb1$^{-/-}$ cells relative to WT, mRNAs for RunX2, alkaline phosphatase, type I collagen, and osteocalcin were reduced 40–90%, all $p < 0.01$, indicating a role of Scarb1 in osteoblast differentiation independent of ACTH. Additionally, in vitro osteoblast differentiation at variable ACTH in WT cells confirmed ACTH increasing bone differentiation, mineralization, alkaline phosphatase, and osteocalcin mRNA at 0–10 nM ACTH, but reduced bone differentiation at 100–1000 nM ACTH. Overall Scarb1$^{-/-}$ animals show inhibited bone formation with age. This may be a mixed effect on direct bone formation and of very high ACTH. Further, this work shows that both ACTH concentration and the HDL receptor Scarb1 play important independent roles in osteoblast differentiation.

Introduction

The scavenger receptor type I, produced by the SCARB1 gene, is the major receptor for high-density lipoprotein (HDL), and an intermediate in production of glycoproteins in the adrenal gland [1].

The role of the HDL receptor in bone formation and turnover is unknown, for the most part. On the other hand, it is established that HDL, via its main protein component apolipoprotein A1, is essential for normal bone formation; its absence decreases osteoblast and increases lipoblast maturation [2, 3]. This effect is affected by diet with increased bone turnover and decreased bone synthesis in apolipoprotein E-deficient mice fed a "Western" diet with high-fat content [4].

In this study, we examined this system further, but instead of targeting the lipoprotein component of HDL, we studied the effects of deleting its main receptor, Scarb1. This model is complex; because of the role of HDL in production of glucocorticoids, the Scarb1 knockout mice have compensatory high adrenocorticotropic hormone (ACTH) levels but normal glucocorticoid levels. We confirmed these findings and hypothesized that ACTH might increase bone mass. because of its role in regulation of bone mass [5] and its promotion of bone survival and vascular development [6] Low-dose injection of ACTH protects against corticosteroid-induced osteonecrosis in rabbits [7]. The effect involves acceleration

✉ Harry C. Blair
hcblair@pitt.edu

1 Veteran's Affairs Medical Center, Pittsburgh, PA 15206, USA

2 Department of Pathology, University of Pittsburgh, Pittsburgh, PA 15261, USA

3 The Mount Sinai Bone Program, Department of Medicine, Icahn School of Medicine at Mount Sinai, New York, NY, USA

4 Department of Anatomy-Histology-Embryology, Unit of Bone and Soft Tissue Studies, University of Patras, School of Medicine, Patras, Greece

of the expression of osteoblast-related genes [8]. Limits on the ACTH effect have been suggested but have not been tested under controlled conditions.

In contrast to other reports, we found that Scarb1 knockout animals in general have reduced bone mass, prominent after 16 weeks of age, without a significant sex affect [9]. The effects on bone differentiation of ACTH in wild-type mesenchymal stem cells (MSC) in vitro confirm the effects of ACTH on bone formation, but only when ACTH is ~10 nM or less. Studies of bone differentiation in vitro show an important direct negative effect of the Scarb1 knockout on osteoblast differentiation, in contrast to other observations [10]. This work shows for the first time, by direct experimental analysis with complete control of variables, that the HDL receptor is required for normal bone differentiation in vivo and in vitro.

Materials and methods

Reagents, cell culture, and treatment

Media and chemicals were from Thermo-Fischer or as stated. Cells were grown in Dulbecco's modified essential medium (DMEM), low glucose (1 g/l) with 10% fetal bovine serum (FBS), penicillin, streptomycin, and amphotericin-B (proliferation medium). Osteoblasts were differentiated from mesenchymal stem cells (MSC). MSC were isolated from mouse femur and tibia as described [11]. The femur and tibia were dissected, and bone marrow flushed with RPMI1640 plus 10% FBS. Erythrocytes were removed with red cell lysis buffer. Cells were plated and incubated for 2 h at 37 °C to remove rapidly adhering fibroblast-like cells. Remaining cells were plated into a new cell culture plate at 1×10^6 cells/cm^2. After 72 h, non-adherent cells were discarded, and adherent cells were washed with phosphate-buffered saline and changed into proliferation medium. To support osteoblast differentiation, cells were grown to confluence and media supplemented with 10 mM 2-glycerol phosphate and 30 μg/ml ascorbic acid, and ACTH if specified. Differentiation media were replaced every 3 days. Cells were in serum-free medium overnight before treatment, when indicated. Empty bones (after bone marrow was flushed for MSC isolation) were cut with razor blades, lysed, and processed for RNA isolation and PCR (see below). Osteoclasts were differentiated from splenocytes. For osteoclast differentiation, murine spleens were removed, gently broken, and passed through a cell strainer. The cells were suspended in RPMI 1640 with 10% heat-inactivated fetal bovine serum. After red cell lysis, the cells were collected and plated at 2×10^5/cm^2 in RPMI 1640 with 10% heat-inactivated fetal bovine serum medium supplemented with 50 ng/ml mouse RANKL, 50 ng/ml mouse CSF, and ACTH if specified for 10 days.

Animals

Scarb1 heterozygotes were obtained from Jackson Labs, Scarb1tm1Kri, and bred to produce wild-type and homozygous knockout animals. The homozygotes are also known as SR-BI KO. The Scarb1$^{-/-}$ mice, on a mixed, but mainly C57 black background, lack the HDL receptor also known as the scavenger receptor class B, member 1 (SRB1). Animals have increased plasma cholesterol (primarily HDL) as compared to wild-type controls and decreased in cholesterol production in the adrenals. It was believed that the decreased adrenal cholesterol and consequent overexpression of ACTH to produce normal cortisol or corticosterone were the main basis of the phenotype, but this proved to be only partly correct (see data below).

Genotyping

Genotyping was performed by PCR using the Jackson Laboratory Protocol 003379B6, with the probes 5'ATCTC AGCCTTAGGCCCTGT, Wild-type Forward Primer; 5' ATAGATTCGCCCTTGTGTCC, Mutant Forward Primer; 5'TCAAACCCTGTGACAACAGC, Common Reverse Primer. The reactions were done together (with all three probes) to produce 140 bp amplicons from the mutant, 262 bp amplicons from the wild type, and both products in the heterozygotes. In brief, a 2-min 94 °C hot start is followed by ten cycles of 94 °C for 20 s, 65 °C for 15 s decreasing 0.5 °C per cycle, and 68 °C for 10 s, followed by 28 cycles of 94 °C 15 s, 60 °C for 15 s, and 72 °C for 10 s. An example of the genotyping is shown in Fig. 1.

Histomorphometry

Static histomorphometry was done by micro-computed tomography (microCT, μCT). Prior to analysis, bone samples for microCT were fixed overnight in 5% formalin and then kept at −20 °C in 70% ethanol. MicroCT was performed using a Skyscan 1172 instrument (Bruker) at 6 μm resolution with 0.5 mm aluminum filter. A 150 mg/ml cutoff was used for bone. Images were reconstructed using the NRecon and InstaRecon software (Bruker). Cross-sectional images were obtained using Dataviewer software and three-dimensional images using the CTvox software (Bruker). Quantitative histomorphometric analysis of lumbar vertebrae bone was performed using the Bruker CTanalyser software.
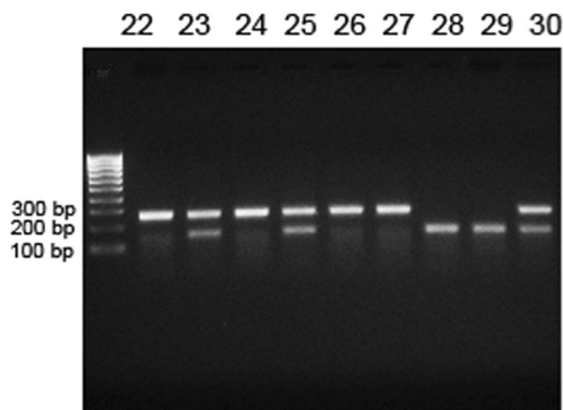
For dynamic histomorphometry, animals were labeled with calcein at 20 μg/g mouse weight 4–5 days before sacrifice and with xylenol orange 80 μg/g mouse weight 2 days later. Unless indicated, thoracic vertebrae 1–3 were used for dynamic histomorphometry and vertebrae 4–6 were used for micro-computed tomography. Bone samples

for fluorescent labels were frozen in blocks at the time of animal sacrifice and cut as frozen sections using carbide blades as described [2]. Bone samples for Hematoxylin and

Eosin (H&E) staining were fixed, dehydrated, paraffin embedded, and cut as 10 μm thick sections using a rotary microtome. Dynamic histomorphometry was measured by a blinded observer.

Serum chemistry

Calcium, phosphate, and cortisol were analyzed using a Beckman clinical system for human studies, relative to standard controls. ACTH and PTH were measured by colorimetric ELISAs (MyBiosource, San Diego, CA) relative to included target standard curves.

RNA isolation and PCR

Total RNA, isolated by oligo dT affinity (RNeasy, Qiagen), was used for complementary DNA (cDNA) synthesis using random hexamers and Moloney murine leukemia virus reverse transcriptase (Superscript III; Invitrogen). Quantitative PCR used an MX3000P instrument (Stratagene) with SYBR green to monitor DNA synthesis. Reactions were run in duplicate, in 25 μl reaction volume with 12.5 μl of pre-mixed dye, NTPs, buffer, and polymerase (SYBR Green Master Mix, Stratagene), to which were added 250 nM primers and 1 μl of first strand cDNA. After 10 min at 95 °C, the mixture was amplified in cycles of 30 s at 95 °C, 30 s at 59 °C, and 1 min at 72 °C. Size and specificity of products was verified by agarose gel electrophoresis. Product abundance relative to controls was calculated assuming linearity to log(initial copies) [12]. Primers are listed in Table 1, except for genotyping sequences shown above.

Fig. 1 Example of genotyping. All animals were genotyped as described in Materials and Methods, using a Jackson Laboratories Kit, by PCR. This is supplied as a kit and uses the probes 5′ATCTC AGCCTTAGGCCCTGT, wild-type forward primer; 5′ATAGA TTCGCCCTTGTGTCC, mutant forward primer; 5′TCAAACCC TGTGACAACAGC, common reverse primer. The reactions were done together (that is, with all three probes) to produce 140 bp amplicons from the mutant, 262 bp amplicons from the wild type, and both products in the heterozygotes. Wild-type animals are showing only the larger band (animals 22, 24, 26, and 27 below), and animals with the deletion showing only the smaller band (28 and 29, below). Animals with both bands are heterozygotes (23, 25, and 30 below). Knockouts were verified by absence of the Scarb1 product, by PCR in osteoblasts (see Fig. 7a below)

Table 1 Mouse primers

ALP NM_007431.2 Product size 131 bp (alkaline phosphatase)	
F - 5′-ATCGGAACAACCTGACTGACCCTT-3′	R - 5′-ACCCTCATGATGTCCGTGGTCAAT-3′
Col1a1 NM_007742.3 Product size 159 bp	
F - 5′-TTCTCCTGGCAAAGACGGACTCAA-3′	R - 5′-AGGAAGCTGAAGTCATAACCGCCA-3′
Osx NM_130458.3 Product size 146 bp (Sp7, osterix)	
F - 5′-GATGGCGTCCTCTCTGCTT-3′	R - 5′-CGTATGGCTTCTTTGTGCCT-3′
RANKL NM_011613.3 Product size 83 bp	
F - 5′-GCTCCGAGCTGGTGAAGAAA-3′	R - 5′-CCCCAAAGTACGTCGCATCT-3′
RunX2 NM_001145920.1 Product size 105 bp	
F - 5′-ATGATGACACTGCCACCTCTGAC-3′	R - 5′-ACTGCCTGGGGTCTGAAAAAGG-3′
ATPa3 NM_178405.3 Product size 163 bp	
F - 5′-TGACCACAAGCTGTCCTTGGATGA-3′	R - 5′-AAGCTGACGACAGAACTTGACCCA-3′
Cathepsin-K NM_007802.3 Product size 174 bp	
F - 5′-CAGCAGAGGTGTGTACTATG-3′	R - 5′-GCGTTGTTCTTATTCCGAGC-3′
TRAP NM_001102405.1 Product size 174 bp	
F - 5′-CACGAGAGTCCTGCTTGTC-3′	R - 5′-AGTTGGTGTGGGCATACTTC-3′
PPARγ NM_011146.3 Product size 100 bp	
F - 5′-CGCTGATGCACTGCCTATGA-3′	R - 5′-AGAGGTCCACAGAGCTGATTCC-3′
SCARB1 NM_016741.2 Product size 149 bp (scavenger receptor class B, member 1)	
F - 5′-TTTGTTGGGGATGAACAACTC-3′	R - 5′-GTCCCATTGATCATGTTACAC-3′
Osteocalcin NM_007541.2, NM_001037939.1 Product size: 118 bp (bone Gla protein, BGLAP)	
F - 5′-ACCATCTTTCTGCTCACTCTGCTG-3′	R - 5′-TATTGCCCTCCTGCTTGGACATGA-3′
Actin NM_007393.3 Product size 275 bp	
F - 5′-GATATCGCTGCGCTGGTCGTC-3′	R - 5′-ACGCAGCTCATTGTAGAAGGTGTG-3′
GAPDH NM_008084.3 Product size 184 bp (glyceraldehyde-3-phosphate dehydrogenase)	
F - 5′-GTTGTCTCCTGCGACTTCA -3′	R - 5′-GGTGGTCCAGGGTTTCTTA-3′

Assay of alkaline phosphatase, mineralization (von Kossa), Oil Red-O, and tartrate-resistant acidic phosphatase (TRAP)

Mineralization was evaluated by silver staining, also called von Kossa staining. Cells were rinsed with PBS and fixed with 4% paraformaldehyde for 5 min. Then cultures were incubated with 2% $AgNO_3$ and placed under UV light for 10 min. The reaction was stopped by 5% sodium thiosulfate then rinsed with water. Alkaline phosphatase activity was determined in citrate-buffered saline at pH 8 using 0.01% naphthol phosphate as substrate and 5 mg/ml of fast blue added, to precipitate the product as an insoluble blue adduct. For the Oil Red-O staining cells were fixed with 4% paraformaldehyde for 5 min. Then cultures were rinsed with 60% isopropanol, stained with freshly prepared Oil Red-O working solution (30 ml of the 0.5% Oil Red-O in isopropanol with 20 ml of distilled water) for 15 min, rinsed with 60% isopropanol, and rinsed with distilled water. Osteoclast differentiation from splenocytes was assessed by tartrate-resistant acidic phosphatase staining using acid phosphatase, leukocyte (TRAP) kit (Sigma-Aldrich). Cells were fixed with 4% paraformaldehyde for 5 min at room temperature and washed two times with distilled water. Then they were stained for tartrate-resistant acid phosphatase (Sigma-Aldrich) according to manufacturer protocol for 90 min at 37 °C away from light. Positive TRAP cells were visualized by a light microscope using 20x objective.

Statistical analysis

GraphPad Prism software was used. Results are mean ± SD, for three or more measurements, as stated. Comparisons of differences used Student's unpaired t-test. Results with $p < 0.05$ were considered significant.
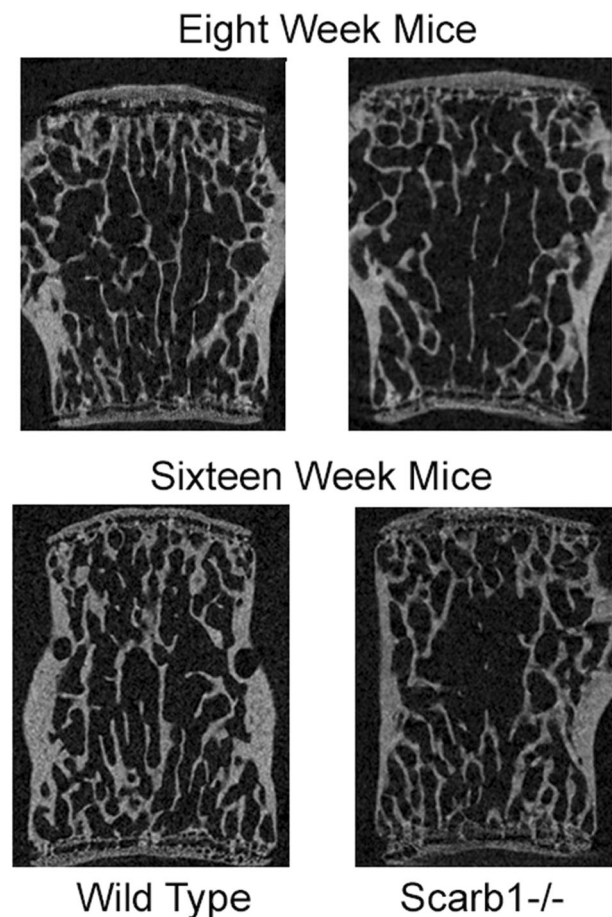
Results

Genotyping

Accurate and comprehensive genotyping was essential; therefore, each animal was genotyped by PCR with primer pairs specific for wild type and the knockout. An example for one litter of animals is shown (Fig. 1); any animal not showing a clear genotype was discarded.
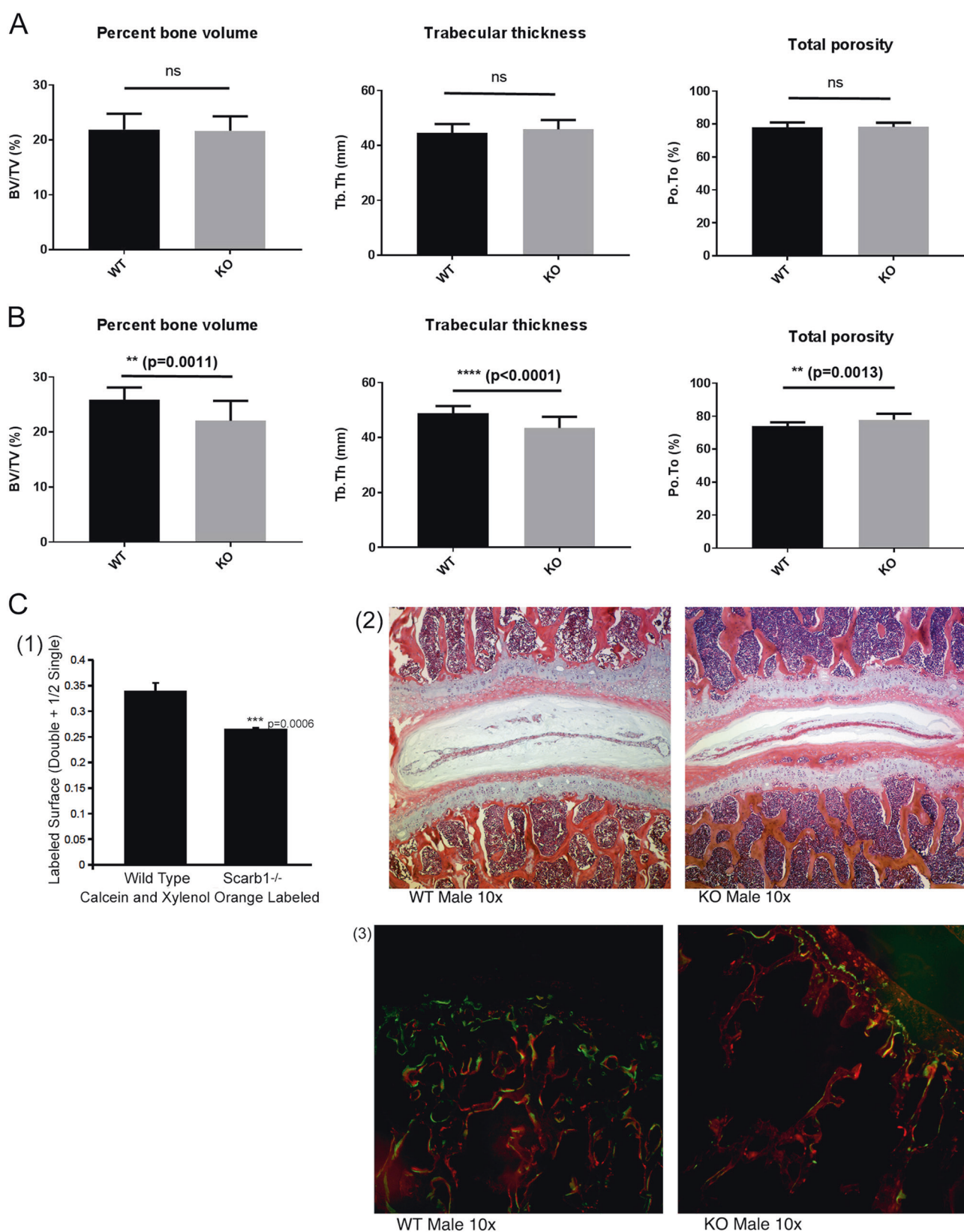
Vertebral bone density and histomorphometry

Sections of vertebral trabecular bone at 8 and 16 weeks are shown in Fig. 2. At 8 or 16 weeks, the central vertebral bone density is less than in the KO, although the quantitative density was significant for the whole vertebrae only at

Fig. 2 Appearance of vertebral trabecular bone at 8 and 16 weeks. Static histomorphometry was done by micro-computed tomography (μCT). MicroCT was performed using a Skyscan 1172 instrument (Bruker) at 6 μm resolution with 0.5 mm aluminum filter. Cross-sectional images were obtained using Dataviewer software and three-dimensional images using the CTvox software (Bruker). In both cases, at 8 and 16 weeks, the central vertebral bone density is less than in the KO although the difference is clearer, and significant for the entire vertebral bodies, at 16 weeks

16 weeks. Static histomorphometry from the μCT is shown in Fig. 3a, b. Analysis reflects an n of 6 for wild type and for the Scarb1 knockout. At 8 weeks, measurements of bone volume/total volume, trabecular thickness, and total porosity were not significantly different between wild type and Scarb1$^{-/-}$. At 16 weeks, BV/TV and trabecular thickness were less in the Scarb1$^{-/-}$ with $p < 0.001$, and porosity was increased in the Scarb1$^{-/-}$. Dynamic histomorphometry by blinded observer showed clear reduction in the bone formation rate, reflected in reduced labeled surface. The interlabel distance did not change (not illustrated). The differences were modest, which was interpreted as probably balanced reduction in bone formation and reduction in bone resorption (see Fig. 5 and Discussion). Equal numbers of males and females were analyzed, and no differences were detected between sexes (not shown).
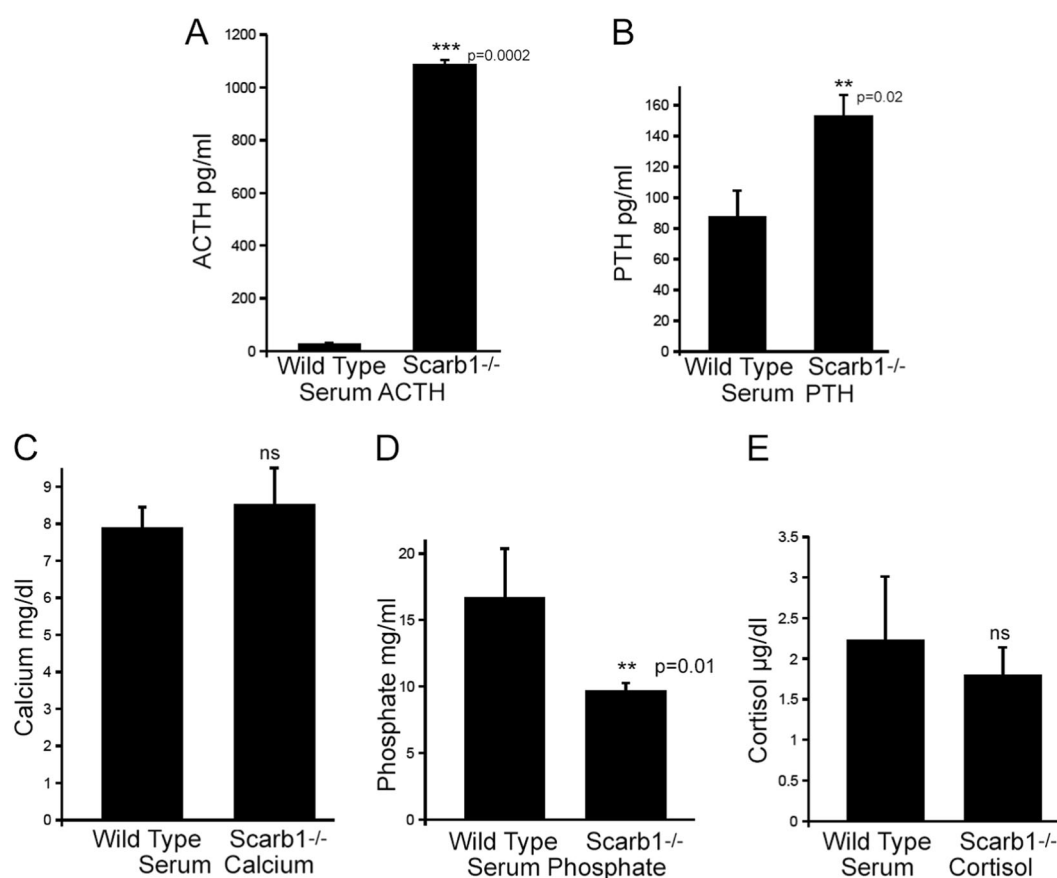
A

Percent bone volume

ns

Trabecular thickness

ns

Total porosity

ns

B

Percent bone volume

** (p=0.0011)

Trabecular thickness

**** (p<0.0001)

Total porosity

** (p=0.0013)

C

(1)

*** p=0,0006

Calcein and Xylenol Orange Labeled

(2)

WT Male 10x   KO Male 10x

(3)

WT Male 10x   KO Male 10x

◀ **Fig. 3** Summary of histomorphometry from µCT and dynamic labeling. Static histomorphometry was done by micro-computed tomography (µCT). MicroCT was performed using a Skyscan 1172 instrument (Bruker) at 6 µm resolution with 0.5 mm aluminum filter. Quantitative histomorphometric analysis of lumbar vertebrae bone was performed using the Bruker CTanalyser software (**a**, **b**). For dynamic histomorphometry, animals were labeled with calcein 4–5 days before sacrifice and with xylenol orange 1–2 days before sacrifice. Bone samples for fluorescent labels (C1, C3) were frozen in blocks at the time of animal sacrifice and cut as frozen section. Bone samples for Hematoxylin and Eosin (H&E) staining (C2) were fixed, dehydrated, paraffin embedded and cut as 10 µm thick sections using a rotary microtome. **c.** $N = 6$ for wild type and for the Scarb1 knockout. **a** Eight-week-old mice. Bone volume/total Volume, trabecular thickness, and total porosity are shown produced using Bruker analysis software. **b** The same parameters as (**a**) at 16-week-old mice. **c** Dynamic labeling on 16-week-old WT and KO males. Shown are the quantity of double + 1/2 single Calcein and Xylenol orange labeled surface area at 16 weeks (1), representative H&E staining for cross sections of vertebral bone (2), and an example of double fluorescent labeled bone subjacent to vertebral disks (3)

Serum chemistry in wild-type and Scarb1$^{-/-}$ mice

Sixteen-week-old mice with an n of 4–6 (Fig. 4) were used. The largest difference between experimental and control groups was extremely high ACTH in the Scarb1$^{-/-}$ mice, on the order of 40 times the median ACTH in the wild-type littermates by ELISA, $p < 0.001$. The Scarb1$^{-/-}$ mice also had increased PTH by ELISA of ~60%, and a similar decrease in phosphate using a clinical assay. Neither calcium nor cortisol levels changed significantly. The increase in PTH was not reflected in increased osteoclastic markers as discussed below. The reason for the deceased phosphate was unclear.
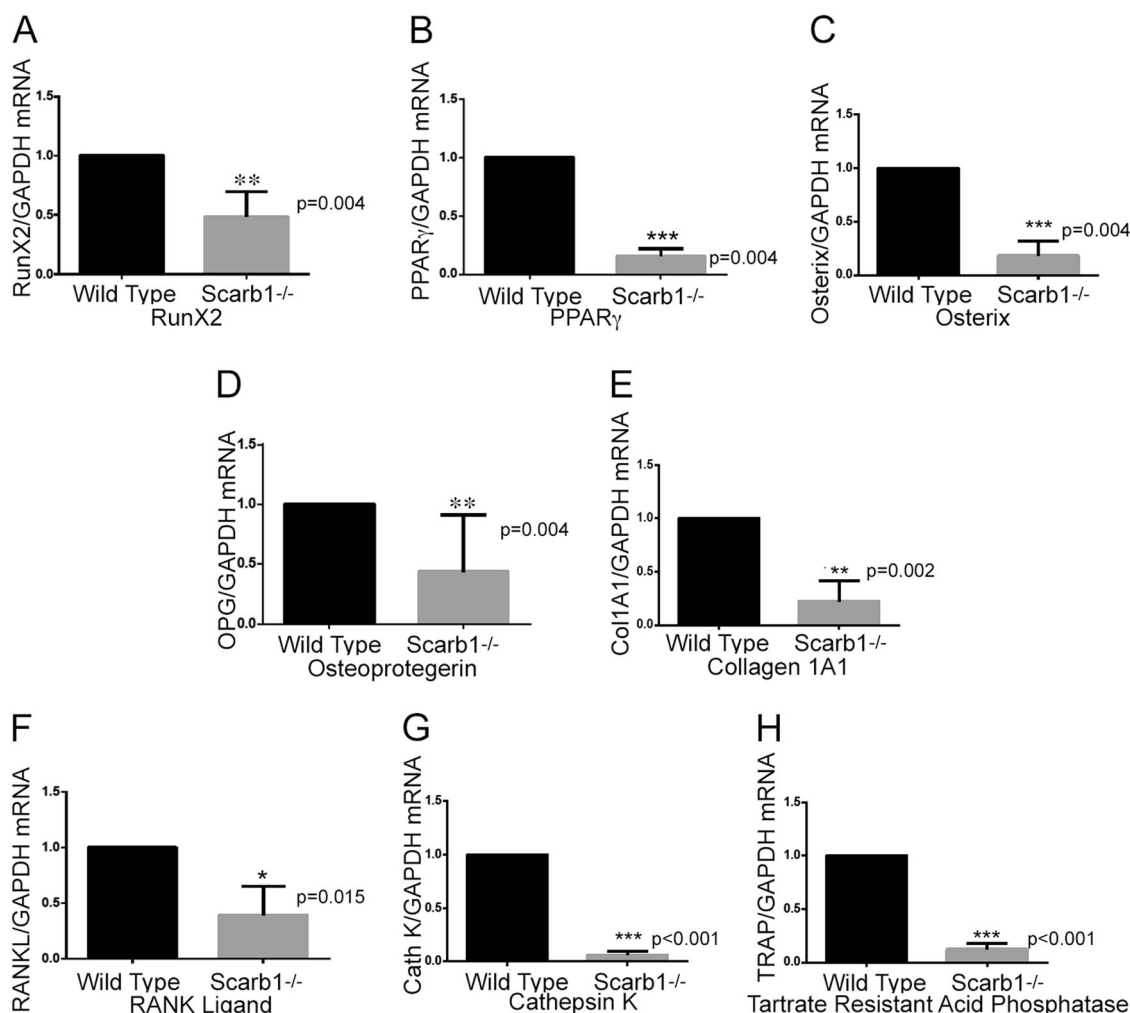
Osteoblast and osteoclast-related messenger RNAs (mRNAs) in cells extracted from bones (femur and tibia)

Osteoblast and osteoclast-related mRNAs in cells extracted from bones (femur and tibia) in vivo were studied by

Fig. 4 Serum chemistry in wild-type and Scarb1 knockout mice. Sixteen-week-old mice, $n = 4$–6, mean ± SD. ACTH (**a**) and PTH (**b**) were measured by colorimetric ELISAs (MyBiosource, San Diego, CA) relative to included target standard curves. Calcium (**c**), phosphate (**d**), and cortisol (**e**) were analyzed using a Beckman clinical system for human studies, relative to standard controls

Fig. 5 PCR assays from cells extracted from bone in vivo. Results in 8-week (shown) and 16-week-old mice were similar. $N = 6$, mean ± SD. Primers are shown in Table 1. Empty bones (after bone marrow was flushed for MSC isolation) were cut with razor blades, lysed, and processed for RNA isolation and quantitative PCR. **a–e** Osteoblast parameters. **f–h** Osteoclast parameters
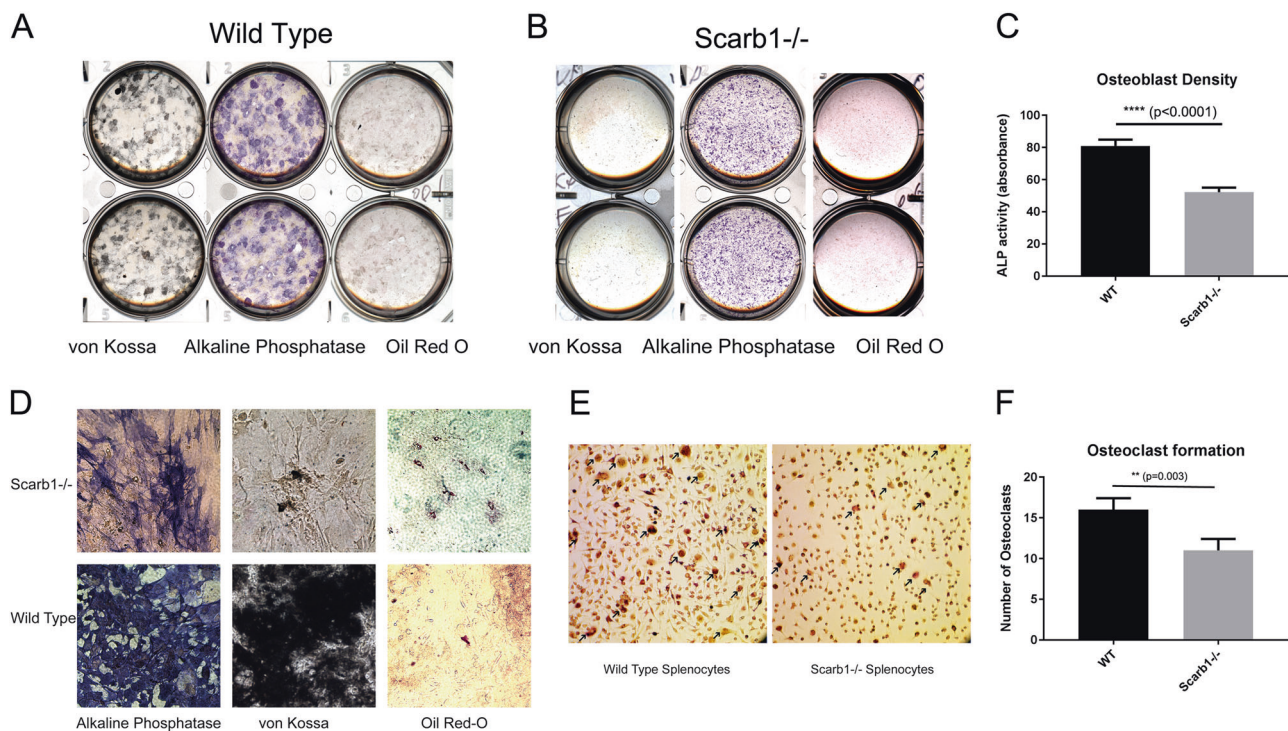
quantitative PCR (Fig. 5). In all cases, bone formation and bone resorption-related parameters were decreased significantly, in most cases with $p < 0.01$. Results of mRNA extracted at 8 weeks (shown) and 16 weeks (not illustrated) were similar.

Osteoblast formation in vitro shows that Scarb1 is essential to normal bone differentiation

Mesenchymal stem cells were isolated from wild-type and Scarb1$^{-/-}$ mice and allowed to differentiate in vitro in medium that supports bone differentiation for 3 weeks (Fig. 6a, b). MSCs were also isolated and differentiated in medium with normal ACTH and PTH concentrations. Cells from wild-type animals showed typical osteoblast differentiation with nodules of alkaline phosphatase and von Kossa labeling cells, and few adipocytes by Oil Red-O. Osteoblast differentiation from Scarb1$^{-/-}$ MSC was reduced.

Quantitative analysis of alkaline phosphatase in osteoblasts differentiated from MSC of wild-type and Scarb1 knockout cells confirms the significant differences (Fig. 6c).

Two examples of differentiation are shown for each assay; several additional MSC lines were tested and the results were uniform in lack of bone nodule formation (not shown). The Scarb1$^{-/-}$ cells showed greatly reduced bone differentiation, and a modest increase in adipocytes seen in microscopy (Fig. 6d). This change is smaller than that seen in the ApoA1 knockout mouse, but the direction of the effect is consistent [2]. In keeping with overall minor effects on bone mass, differentiation of osteoclasts was also reduced (Fig. 6e, f). These results indicate that Scarb1 is required for normal osteoblast differentiation under conditions where ACTH and other serum factors are not relevant. Equal numbers of males and females were analyzed; no differences between sexes were detected (not illustrated).

Fig. 6 Effects of Scarb1 independent of ACTH demonstrated in vitro. **a**, **b** von Kossa, alkaline phosphatase, and Oil Red-O staining of wild type and Scarb1 knockout MSC differentiated into osteoblasts for 3 weeks in vitro. Two representative cultures of each type are shown. Differentiation of several mesenchymal stem cell preparations of each type was consistent. Whole wells of six-well plates are shown (3.5 cm). **a** Wild-type cells. **b** Scarb1 knockout cells. **c** Quantitative alkaline phosphatase in osteoblasts differentiated 3 weeks from MSC of wild-type and Scarb1 knockout cells. Mean ± SD, $N = 4$, $p < 0.01$. **d** Microscopic appearance of alkaline phosphatase, von Kossa, and Oil Red-O staining of wild type and Scarb1 knockout MSC differentiated into osteoblasts for 3 weeks in vitro. Fields are 200 microns wide. **e** Microscopic appearance of tartrate-resistant acidic phosphatase (TRAP) staining of osteoclasts differentiated from splenocytes of wild type and Scarb1 knockout for 10 days in vitro. Fields shown are 400 microns wide. Examples of osteoclasts are indicated with arrows. **f** The number of osteoclasts formed from splenocytes of Scarb1 KO mice and of wild-type mice

Confirmation of defective osteoblast and osteoclast differentiation in tissue culture by quantitative PCR using mRNA from wild type and Scarb1$^{-/-}$ differentiated MSC and splenocytes, respectively, by PCR. We showed unequivocally that genes required for osteoblast and osteoclast formation are expressed at much lower levels in the Scarb1$^{-/-}$ cells (Fig. 7). Differences were highly significant for all osteoblast markers in MSC differentiated into osteoblasts (Fig. 7b–e), and in most cases significant for osteoclast markers in splenocytes differentiated into osteoclasts (Fig. 7f–h), although there was more variability in osteoclast markers. These experiments also confirmed the Scarb1 knockout (Fig. 7a).

Effects of ACTH independent of Scarb1

In addition, we studied the effects of ACTH on bone differentiation over a very broad range of ACTH concentrations in wild-type cells (Fig. 8). This work showed strong support of bone differentiation up to 10 nM, whether by mineralization (A), osteocalcin (B), or alkaline phosphatase (C) assays, with declines in osteoblast differentiation at about 100 nM and above. This strongly su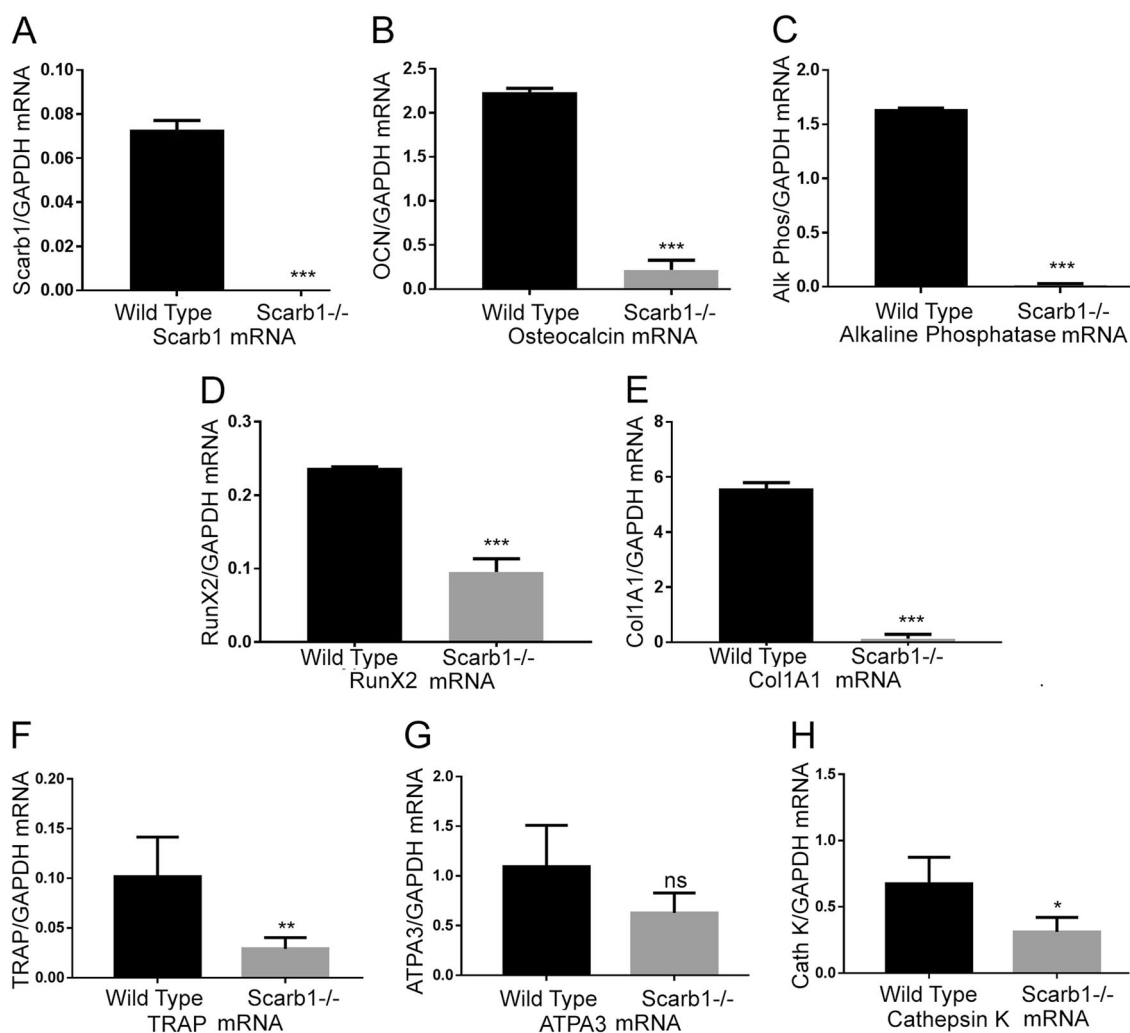pports a limit on support of bone formation, and possibly survival, on ACTH concentration. We also analyzed the effects of ACTH on splenocytes differentiated into osteoclasts for 10 days. While 10 nM, and 100 nM ACTH did not significantly change the number of osteoclasts, 1000 nM ACTH significantly reduced osteoclast formation, probably due to toxicity.

Discussion

This study re-evaluated the effect of knockout of the HDL receptor Scarb1 on bone phenotype. There are two important findings and some secondary effects. First, lack of the Scarb1 receptor, as expected, caused high ACTH, much higher ACTH than the 4–5-fold elevation initially reported [13]. This is likely due to the apparent slow induction of the phenotype; our main evaluation was at 16 weeks of age.

High ACTH was expected to correlate with increased bone formation [6], but reduced bone mass and greatly reduced bone formation and resorption markers were consistently seen. Bone differentiation in the Scarb1$^{-/-}$ animals is greatly diminished in vitro as well as in vivo. The in vitro

Fig. 7 Expression of osteoblast and osteoclast-related genes in tissue culture by PCR. **a** Confirmation of the Scarb1 knockout. **b–e** Osteoblast developmen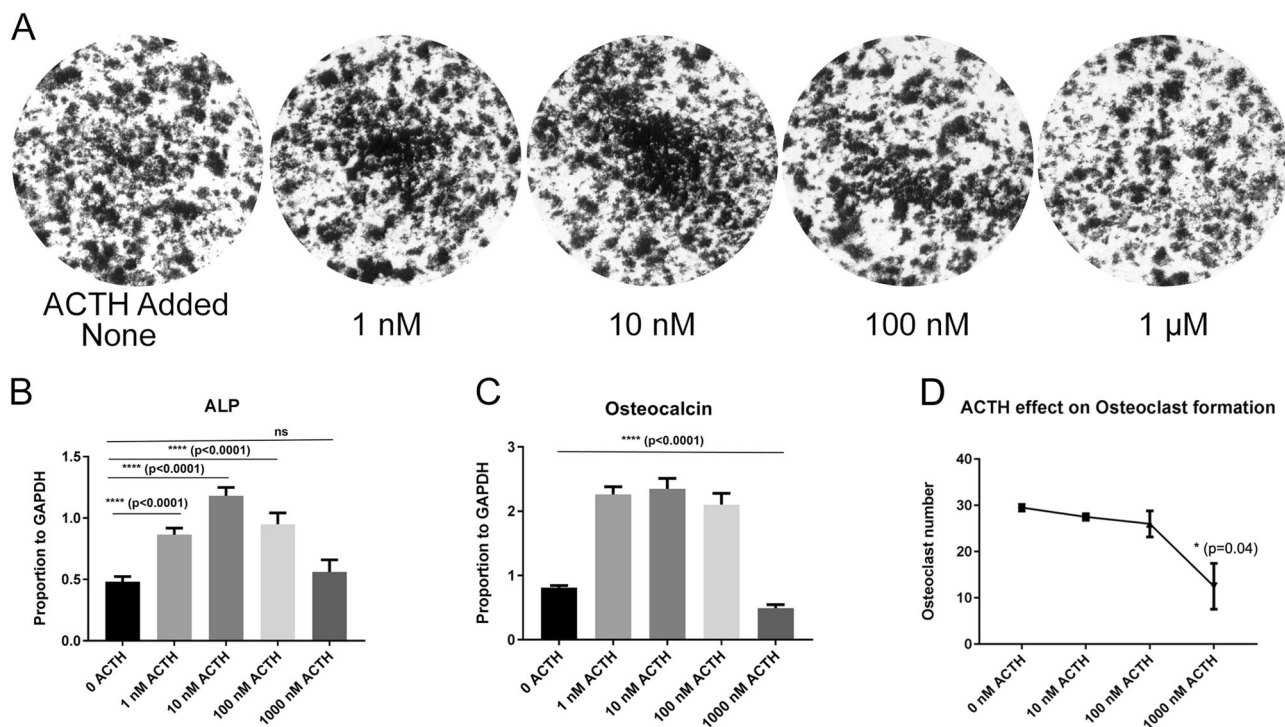t gene mRNAs. Osteoblasts were differentiated from MSC for 3 weeks in vitro. **f–h** Osteoclast development gene mRNAs. Osteoclasts were differentiated from splenocytes for 10 days in vitro

findings, in medium without effects of serum changes including in ACTH, imply strongly that the HDL receptor Scarb1$^{-/-}$ might be essential for normal bone formation and that many secondary effects occur. This contrasts with early reports that osteoblast differentiation might be increased, with negative effects on terminal osteocyte differentiation [10]. In contrast, we observed general decreased osteoblast differentiation and bone resorption (Figs. 6 and 7).

Low doses of ACTH and ACTH-regulated VEGF (vascular endothelial growth factor) were shown to protect against glucocorticoid-induced osteonecrosis of bone in rabbit and canine models, and potential protection for lumbar bone mineral density in patients with Cushing's disease [7, 14, 15]. However, high ACTH induced osteonecrosis, typically also with elevated glucocorticoids, in pituitary tumors [16, 17]. This situation is complex but suggested that there is a dose-dependency for ACTH effects on bone formation. We tested this in vitro by adding a wide range of ACTH to MSC

differentiating into osteoblast (Fig. 8), which showed strong support of bone differentiation up to 10 nM, with declines in osteoblast differentiation at about 100 nM and above. Thus, it is important in contemplating ACTH for protection of bone that the dose be considered, and the low-dose therapy effective [2] might be a good starting point.

Potentially the most important underlying physiology is that high-density lipoprotein is a key factor in bone differentiation. Clues to this without the ACTH effects come from ApoA1 knockout work [2, 3], apolipoprotein A1 being the main lipoprotein in high-density lipoprotein. In keeping, the HDL receptor Scarb1, when absent, severely affects bone formation in vivo and in vitro, the effects in vitro eliminating the possibility of serum effects (Figs. 3–7). This has long been suspected from correlative data [18, 19]. Difficulties with the hypothesis include controlling both HDL and secondary effects as variables; the Scarb1$^{-/-}$ model in vitro may allow characterization of what effects

Fig. 8 Dose-dependent effect of ACTH on osteoblast and osteoclasts differerentiating. **a–c** Effects of 0, 1, 10, 100, and 1000 nM ACTH on wild type MSC differentiated into osteoblasts for 3 weeks. **a** Mineralization (von Kossa stain). Shown are 3 cm wide images of wells from a six-well plate. **b** Expression of osteocalcin by PCR. **c** Expression of alkaline phosphatase by PCR. **d** Effects of 0, 10, 100, and 1000 nM ACTH on wild-type splenocytes differentiated into osteoclasts for 10 days. Osteoclasts numbers from two different cultures were calculated

are due to HDL lipid and cholesterol delivery for bone synthesis, and how secondary induction of bone-related genes are controlled. This will await further work.

Why do defects in vivo continue in vitro? One of the most curious findings is reduction of both osteoclast differentiation from splenocytes, and osteoblast formation from MSC of Scarb$^{-/-}$ animals in vitro. In the case of the splenocytes, the cells are direct from low turnover bone so this might be a simple effect on harvesting committed cells. On the other hand, MSC are isolated and grown in normal medium for at least a month, and then differentiated in vitro for 3 weeks in normal medium. There are two main possibilities, neither exclusive, for why these MSC show reduced osteoblastic differentiation. One is that the MSC subpopulations have been changed durably in the Scarb1$^{-/-}$ animals during growth and differentiation. Variation of MSC subtypes is known to regulate osteoblast formation in other contexts [20, 21]. Another possibility is that Scarb1$^{-/-}$ itself is a receptor modifying many variables involved in bone formation (Fig. 7). To resolve the issues, it will be necessary to characterize the detailed MSC subtypes in the Scarb1$^{-/-}$ animals, and to study HDL-dependent signaling in osteoblasts. These issues are potentially very important but are beyond the scope of the present work.

In conclusion, the HDL receptor Scarb1 is essential for normal bone formation in vivo and in vitro. It remains uncertain the degree to which the effects are due to lack of lipid [22] and cholesterol [23, 24] to supply for the high metabolic rate of bone synthesis. This is an extremely important issue involving the basic metabolism of bone. Further molecular work and analysis of defects in the Scarb1$^{-/-}$ animal will play an important role in deciding these issues.

Compliance with ethical standards

References

1. Shen WJ, Hu J, Hu Z, Kraemer FB, Azhar S. Scavenger receptor class B type I (SR-BI): a versatile receptor with multiple functions and actions. Metabolism. 2014;63:875–86.

2. Blair HC, Kalyvioti E, Papachristou NI, Tourkova IL, Syggelos SA, Deligianni D, et al. Apolipoprotein A-1 regulates osteoblast

and lipoblast precursor cells in mice. Lab Invest. 2016;96: 763–72.

3. Papachristou NI, Blair HC, Kypreos KE, Papachristou DJ. High-density lipoprotein (HDL) metabolism and bone mass. J Endocrinol. 2017;233:R95–107.

4. Papachristou NI, Blair HC, Kalyvioti ES, Syggelos SA, Karavia EA, Kontogeorgakos V, et al. Western-type diet differentially modulates osteoblast, osteoclast, and lipoblast differentiation and activation in a background of APOE deficiency. Lab Invest. 2018;98:1516–26.

5. Isales CM, Zaidi M, Blair HC. ACTH is a novel regulator of bone mass. Ann N Y Acad Sci. 2010;1192:110–6.

6. Martineau C, Martin-Falstrault L, Brissette L, Moreau R. The atherogenic Scarb1 null mouse model shows a high bone mass phenotype. Am J Physiol Endocrinol Metab. 2014;306:E48–57.

7. Zaidi M, Sun L, Robinson LJ, Tourkova IL, Liu L, Wang Y, et al. ACTH protects against glucocorticoid- induced osteonecrosis of bone. Proc Natl Acad Sci USA. 2010;107:8782–7.

8. Tourkova IL, Liu L, Sutjarit N, Larrouture QC, Luo J, Robinson LJ, et al. Adrenocorticotropic hormone and 1,25-dihydroxyvitamin D(3) enhance human osteogenesis *in vitro* by synergistically accelerating the expression of bone-specific genes. Lab Invest. 2017;97:1072–83.

9. Martineau C, Martin-Falstrault L, Brissette L, Moreau R. Gender- and region-specific alterations in bone metabolism in Scarb1-null female mice. J Endocrinol. 2014;222:277–88.

10. Martineau C, Kevorkova O, Brissette L, Moreau R. Scavenger receptor class B, type I (Scarb1) deficiency promotes osteo-blastogenesis but stunts terminal osteocyte differentiation. Physiol Rep. 2014;2:e12117.

11. Dobrowolski SF, Tourkova IL, Robinson LJ, Secunda C, Spridik K, Blair HC. A bone mineralization defect in the Pah(enu2) model of classical phenylketonuria involves compromised mesenchymal stem cell differentiation. Mol Genet Metab. 2018;125:193–9.

12. Bustin SA. Absolute quantification of mRNA using real-time reverse transcription polymerase chain reaction assays. J Mol Endocrinol. 2000;25:169–93.

13. Hoekstra M, Meurs I, Koenders M, Out R, Hildebrand RB, Kruijt JK, et al. Absence of HDL cholesteryl ester uptake in mice via SR-BI impairs an adequate adrenal glucocorticoid-mediated stress response to fasting. J Lipid Res. 2008;49:738–45.

14. Guo W, Li F, Zhu C, Wang B, Wang K, Dai C, et al. Effect of hypercortisolism on bone mineral density and bone metabolism: a potential protective effect of adrenocorticotropic hormone in patients with Cushing's disease. J Int Med Res. 2018;46:492–503.

15. Dailiana ZH, Stefanou N, Khaldi L, Dimakopoulos G, Bowers JR, Fink C, et al. Vascular endothelial growth factor for the treatment of femoral head osteonecrosis: An experimental study in canines. World J Orthop. 2018;9:120–9.

16. Premkumar M, Dhanwal DK, Mathews S, Garg A, Sahoo S, Mahamine K, et al. Avascular osteonecrosis of femoral head in a postoperative patient of pituitary Cushing's disease. J Assoc Physicians India. 2013;61:413–5.

17. Kyriacou A, Stepien KM, Issa B. Urinary steroid metabolites in a case of florid Ectopic Cushing's syndrome and clinical correlations. Hormones (Athens). 2016;15:540–7.

18. Ackert-Bicknell CL. HDL cholesterol and bone mineral density: is there a genetic link? Bone. 2012;50:525–33.

19. Tintut Y, Demer LL. Effects of bioactive lipids and lipoproteins on bone. Trends Endocrinol Metab. 2014;25:53–9.

20. Park D, Spencer JA, Koh BI, Kobayashi T, Fujisaki J, Clemens TL, et al. Endogenous bone marrow MSCs are dynamic, fate-restricted participants in bone maintenance and regeneration. Cell Stem Cell. 2012;10:259–72.

21. Feigenson M, Eliseev RA, Jonason JH, Mills BN, O'Keefe RJ. PGE2 receptor subtype 1 (EP1) regulates mesenchymal stromal cell osteogenic differentiation by modulating cellular energy metabolism. J Cell Biochem. 2017;118:4383–93.

22. Kushwaha P, Wolfgang MJ, Riddle RC. Fatty acid metabolism by the osteoblast. Bone. 2018;115:8–14.

23. Li H, Guo H, Li H. Cholesterol loading affects osteoblastic differentiation in mouse mesenchymal stem cells. Steroids. 2013;78:26–33.

24. Viccica G, Vignali E, Marcocci C. Role of the cholesterol biosynthetic pathway in osteoblastic differentiation. J Endocrinol Invest. 2007;30(6 Suppl):8–12.